



Anal. Bioanal. Chem. Res., Vol. 7, No. 2, 151-160, June 2020.

DMOF-1 Assessment and Preparation to Electrochemically Determine Hydrazine in Different Water Samples

Peyman Mohammadzadeh Jahani^{a,*}, Somayeh Tajik^{b,*}, Mohammad Reza Aflatoonian^{c,b}, Reza Alizadeh^d and Hadi Beitollahi^e

^a*School of Medicine, Bam University of Medical Sciences, Bam, Iran*

^b*Research Center for Tropical and Infectious Diseases, Kerman University of Medical Sciences, Kerman, Iran*

^c*Leishmaniasis Research Center, Kerman University of Medical Sciences, Kerman, Iran*

^d*Department of Chemistry, Faculty of Science, Qom University, Qom, Iran*

^e*Environment Department, Institute of Science and High Technology and Environmental Sciences, Graduate University of Advanced Technology, Kerman, Iran*

(Received 18 May 2019 Accepted 17 August 2019)

Hydrazine has been identified as a carcinogenic mutagenic, hepatotoxic, and neurotoxin material. A metal-organic framework with tetragonal symmetry, DMOF-1 ($Zn_2(bdc)_2dabco$) was synthesized by a versatile and facile technique, followed by its efficient development and validation as hydrazine electrochemical sensor. Differential pulse voltammetry (DPV), linear sweep voltammetry (LSV), and cyclic voltammetry (CV) techniques were used as diagnostic techniques. Scanning electron microscopy (SEM) and x-ray diffraction (XRD) were also used to characterize the MOF. In the electro-oxidation of hydrazine, there was a highly catalytic activity shown by the modified electrode. In addition, there was a greater signal response, compared to the unmodified electrode, which was primarily attributed to the large active surface area provided by DMOF-1. The detection limit for hydrazine, linear range, and sensor sensitivity were reported to be 0.02 μM , 0.09-400.0 μM , and 0.0863 $\mu A/\mu M^{-1}$, respectively. Based on the results, the amplified sensor was able to properly analyze hydrazine in different samples of water.

Keywords: DMOF-1, Hydrazine, Electrochemical sensor, Modified electrode, Screen printed electrode

INTRODUCTION

With a broad range of agricultural, medical, military, and industrial uses, hydrazine (N_2H_4) is a strong reducing agent and an extremely reactive base [1,2]. Easily absorbed via inhalation, skin, and oral exposure routes, hydrazine is a toxic and volatile material. Moreover, it has been identified as a carcinogenic mutagenic, hepatotoxic, and neurotoxin material [3-6]. As such, many studies have focused on the formation of novel techniques for initial hydrazine

detection.

Electrochemistry, liquid chromatography, spectrophotometry, capillary electrophoresis, flow injection analysis, and gas chromatography-mass spectrometry (GC-MS) are among numerous approaches formerly created to measure the hydrazine's concentration level [7-14]. Nevertheless, these methods have some shortages in terms of being used in real-time or in-situ measurements, including high cost, difficult application and complicated operation. However, owing to its high sensitivity, simple operation, and rapid response, the electrochemical technique is one of the most desirable methods.

Patterned mini-electrode systems with working,

*Corresponding authors. E-mail: mjpeyman@yahoo.com; tajik_s1365@yahoo.com

reference, and auxiliary electrodes, screen printed electrodes (SPEs) have become very popular in electrochemical sensors owing to their easy production and portability, high sensitivity, low cost, and fast response [15]. Several compounds have been discovered by the extensive application of SPE-based electrochemical sensors [16-20].

Nevertheless, the slow kinetics and surface fouling onto electrochemical devices limit the direct oxidation of electroactive compounds at conventional electrodes. In addition, other shortages of original electrodes as an electrochemical sensor for detection of electroactive compounds include high over-potential at electrodes, stability over a wide range of solution compositions, low sensitivity, and reproducibility [21]. Therefore, scholars have employed electrode surface modification at a broad range to deal with these shortages and enhance the features of the electrode surface in order to determine some pharmaceutical, biological, and environmental compounds [22-32].

In today's basic science, one of the most attractive disciplines is nanoscience. Different attractive fields drive a great interest in nanoscience, thereby forming a novel industrial revolution [33]. According to the research, the modified nanomaterials can enhance the electrochemical sensors' sensitivity [34-42].

Belonging to the family of metal-organic frameworks (MOFs), DMOF-1 (also represented as $Zn_2(bdc)_2dabco$) is a crystalline nanoporous coordination polymer consisting of the Zn_2 metal clusters connected by four benzene-(1,4)-dicarboxylate (bdc) residues to create stretched planar sheets. In the third dimension, the adjacent sheets are linked by 1,4-diazabicyclo [2.2.2]octane (dabco) linkers. The alignment of the phenyl rings in the $Zn_2(bdc)_2$ sheets is vertical to their plane on average [43].

Considering the metal ions are synchronized to organic ligands to create inflexible 3D frameworks with special characteristics (*e.g.*, chemical tenability, high porosity, and high accessible surface area), MOFs have been recognized as a new category of crystalline porous materials since the last decade [44]. MOFs have exhibited proper uses in different industrial and research fields, such as gas separation/storage, magnet, sensing and heterogeneous catalysis, due to their brilliant features [45]. As such, MOFs can be essentially motivating and practically valuable in the

alteration of electrochemical sensors [46].

Preparation of a DMOF-1/SPE and its function in electro-oxidation determining of hydrazine in aqueous solutions are described in the current research. Moreover, the analytical performance of the modified electrode is evaluated to determine hydrazine in different water samples.

EXPERIMENTAL

Chemicals and Apparatus

An Autolab potentiostat/galvanostat (PGSTAT 302N, Eco Chemie, the Netherlands) was applied for measuring electrochemicals. General Purpose Electrochemical System (GPES) software was employed to control conditions of experiments.

The screen-printed electrode (DropSens, DRP-110, Spain) includes 3 main sections that contain a silver pseudo-reference electrode, a graphite working electrode, and graphite counter electrode. The pH was measured by a Metrohm 710 pH meter.

Hydrazine and all the remaining reagents had an analytical grade. They have been prepared via Merck (Darmstadt, Germany). Orthophosphoric acid and the related salts, above the pH range of 2.0-9.0, were used for preparing the buffer solutions.

Preparation of DMOF-1

After adding 0.1 g of 1,4-benzene dicarboxylic acid and 0.035 g of 1,4-diazabicyclo[2,2,2] octane as ligands to DMF (25 ml), the compound was reserved in the ultrasonic bath (duration = 10 min). Combining acetic acid (0.57 ml) and zinc acetate (0.132 g) with DMF (10 ml) resulted in the formation of the metal solution. Afterwards, the integrated solution of ligand and metal was boiled at 120 °C for 48 h. After washing the white precipitate with DMF, it was dried for 24 h at 60 °C.

Preparation of the Electrode

DMOF-1 has been used to coat the bare screen-printed electrode. A stock solution of DMOF-1 in 1 ml of aqueous solution was prepared by distributing 1 mg of DMOF-1 *via* ultra-sonication for 30 min, whereas 5 μ l of aliquots of the DMOF-1 suspension solution was cast on carbon working electrodes. Then, we waited until the solvent was

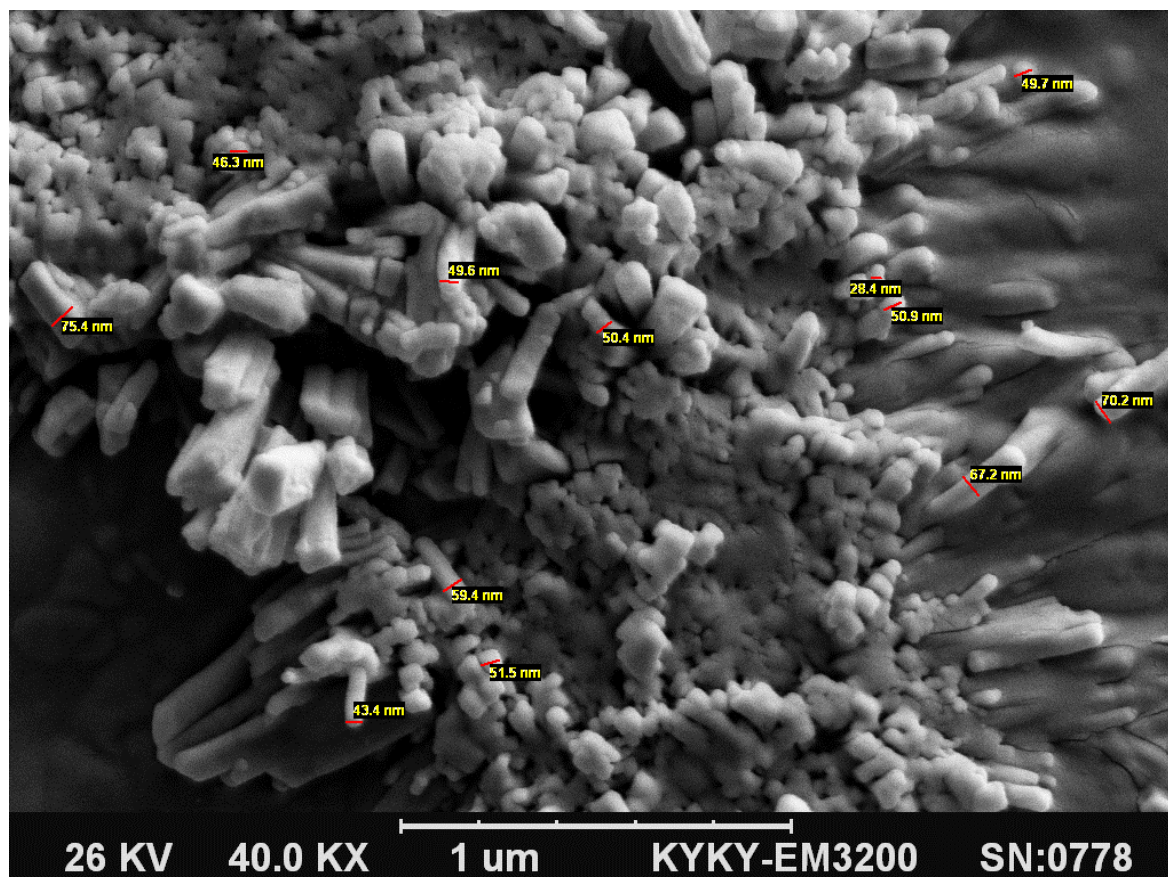


Fig. 1. SEM image of DMOF-1.

evaporated at room temperature.

RESULTS AND DISCUSSION

Microscopic Area of DMOF-1/SPE

The microscopic areas of the DMOF-1/SPE and the bare SPE were obtained by CV using 1 mM $K_3Fe(CN)_6$ as a probe at different scan rates. For a reversible process, the Randles-Sevcik formula [47] was used:

$$i_{pa} = 2.69 \times 10^5 n^{3/2} A C_0 D_R^{1/2} v^{1/2} \quad (1)$$

where i_{pa} refers to the anodic peak current, n the electron transfer number, A the surface area of the electrode, D_R the diffusion coefficient, C_0 the concentration of $K_3Fe(CN)_6$ and v is the scan rate. For 1 mM $K_3Fe(CN)_6$ in the 0.1 M

KCl electrolyte: $n = 1$ and $D_R = 7.6 \times 10^{-6} \text{ cm}^2 \text{ s}^{-1}$, then from the slope of the $i_{pa}-v^{1/2}$ relation, the microscopic areas were calculated. In DMOF-1/SPE, the electrode surface was found to be 0.14 cm^2 which was about 4.46 times greater than the bare SPE.

Morphology and Structure of DMOF-1

The morphology of as-synthesized product was characterized by scanning electron microscopy (SEM) (Fig. 1). The SEM image of D-MOF1 shows that the nano rods of the synthesized MOF are below 100 nm. Also, the nano rods were aligned successfully. The result shows that the high surface area will achieve because of the nano porous structure of MOF and nano rods of D-MOF1.

The powder XRD pattern of DMOF-1 is illustrated in Fig. 2. The result shows some sharp peaks confirming the

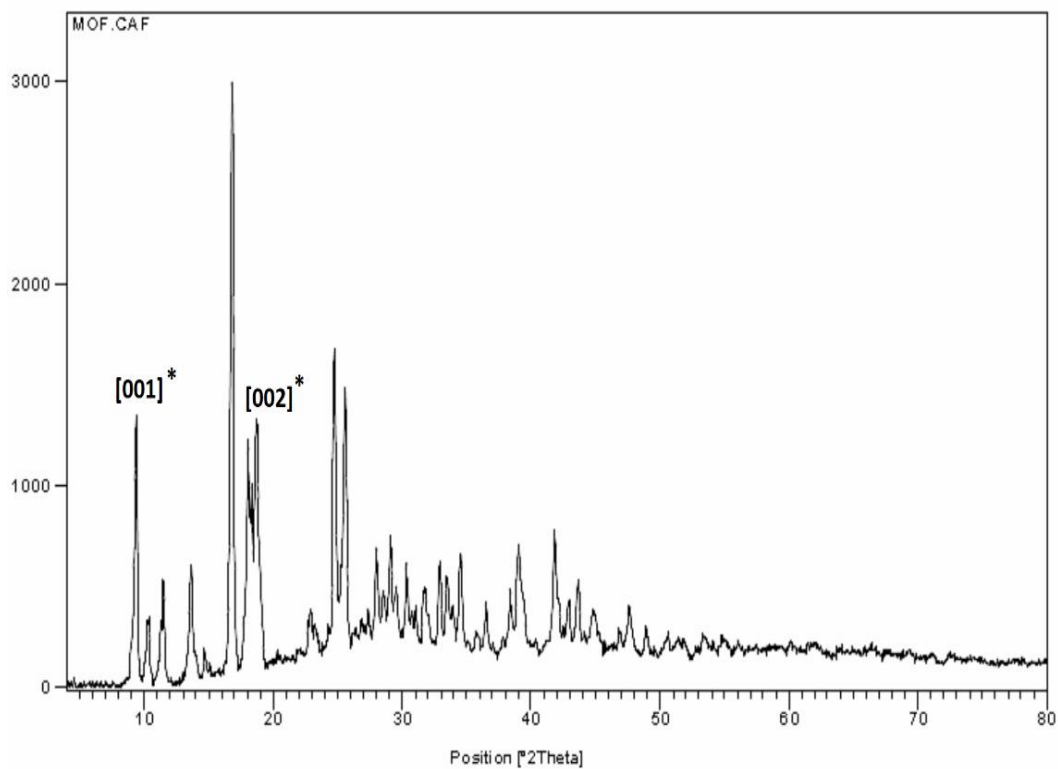


Fig. 2. The XRD pattern of DMOF-1.

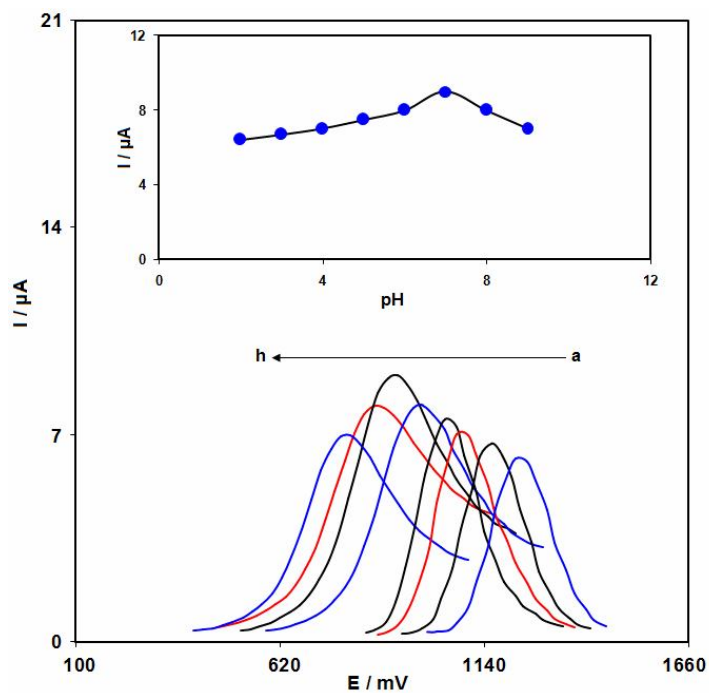


Fig. 3. DPV (at 50 mV s^{-1}) of DMOF-1/SPE at various buffered pHs, a-h correspond to 2.0, 3.0, 4.0, 5.0, 6.0, 7.0, 8.0 and 9.0 pHs, respectively. Inset: Plot of I vs. pH.

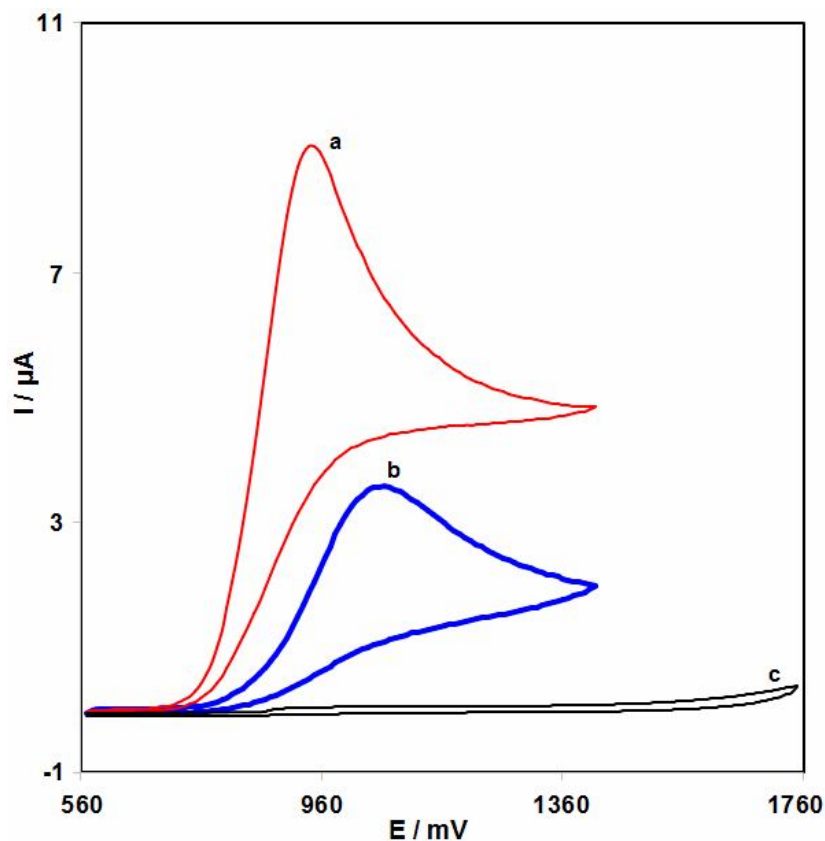


Fig. 4. CVs of (a) DMOF-1/SPE and (b) bare SPE in 0.1 M PBS (pH 7.0) in the presence of 100.0 μM hydrazine, and (c) DMOF-1/SPE in 0.1 M PBS (pH 7.0) in the absence of hydrazine. In all cases the scan rate is 50 mV s^{-1} .

formation of nano structure of D-MOF-1. Also, comparison of XRD pattern of the synthesized D-MOF-1 with simulated patterns in the literatures demonstrates that the D-MOF-1 was synthesized correctly [48,49].

Electrochemical Behaviour of Hydrazine at the Surface of Different Electrodes

The electrochemical behaviour of hydrazine depends on the pH value of the aqueous solution. Thus, it is essential to optimize the solution pH in order to gain more useful results for electro-oxidation of hydrazine. Therefore, hydrazine electrochemical behaviour was examined in 0.1 M PBS at distinct pH values (2.0-9.0) at the DMOF-1/SPE surface by voltammetry (Fig. 3). The results indicated more advantages of neutral conditions for hydrazine electro-oxidation at the DMOF-1/SPE surface in comparison to the basic or acidic

medium. Here, pH 7.0 was selected as an optimal pH for hydrazine electro-oxidation at DMOF-1/SPE surface (Fig. 3 inset).

Figure 4 shows responses of CV to electro-oxidation of 100.0 μM hydrazine at the unmodified SPE (curve b) and DMOF-1/SPE (curve a). The peak potential occurs at 950 mV due to hydrazine oxidation, which is around 125 mV more negative than the unmodified SPE. Furthermore, DMOF-1/SPE exhibits more anodic peak currents for hydrazine oxidation than those of the unmodified SPE. This showed a significant improvement of the electrode performance toward hydrazine oxidation by modification of SPE changing the constant SPE with DMOF-1.

Also, DMOF-1/SPE in the absence of hydrazine in 0.1 M PBS pH 7.0 (Curve c) showed no peak current. According to the literature, MOFs have a large surface area

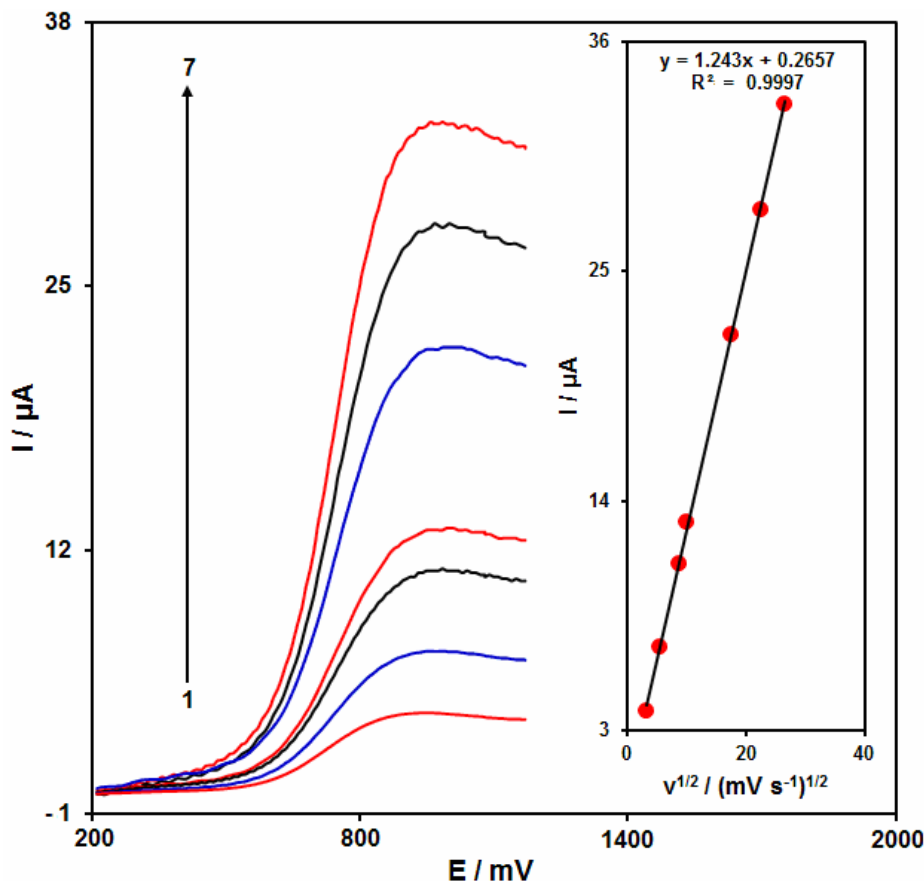


Fig. 5. LSVs of DMOF-1/SPE in 0.1 M PBS (pH 7.0) consisting of 100.0 μM of hydrazine at different scan rates. Values 1-7 are in agreement with 10, 30, 75, 100, 300, 500 and 700 mV s⁻¹, respectively. Inset: Variation of anodic peak current vs. v^{1/2}.

and they can be useful in electrochemistry because of the electrochemical activity of the metal ions and the well-ordered porous skeleton [50]; the features are in accordance to our results.

Influence of Scan Rate

Researchers investigated the influence of the rates of potential scan on hydrazine oxidation current (Fig. 5). Findings indicated induction of enhancement in the peak current by the increase in potential scan rate. Additionally, diffusion in oxidation processes are monitored, as inferred by the linear dependence of the anodic peak current (I_p) on the square root of the potential scan rate (v^{1/2}) for hydrazine [47].

Calibration Plot and Detection Limit

The electro-oxidation peak currents of hydrazine at DMOF-1/SPE surface can be applied to detect hydrazine in the solution. Since the increased sensitivity and more suitable properties for analytical utilizations are considered as the benefits of differential pulse voltammetry (DPV), DMOF-1/SPE in 0.1 M PBS consisting of different distinct concentrations of hydrazine was used to conduct DPV experiments (Fig. 6). It was found that the peak currents of hydrazine oxidation at DMOF-1/SPE surface linearly depended on hydrazine concentrations above the range of 0.09-400.0 μM, while determination limit (3σ) achieved was 0.02 μM.

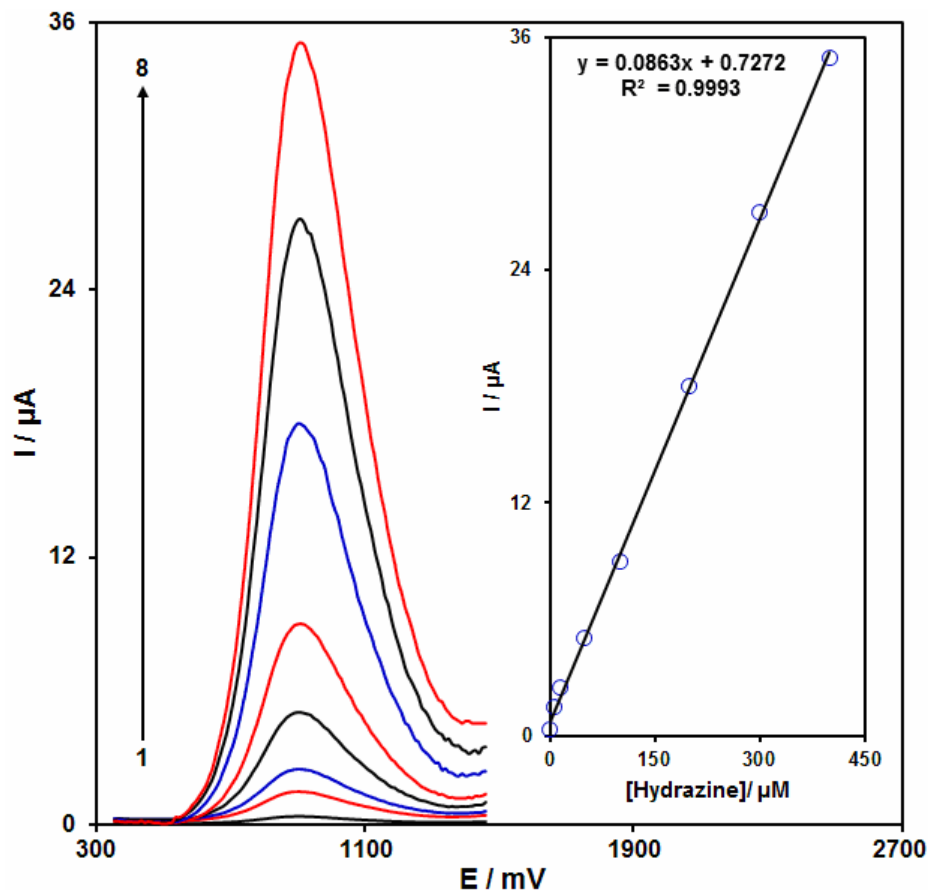


Fig. 6. DPVs of DMOF-1/SPE in 0.1 M PBS (pH 7.0) composing of various concentrations of hydrazine. Values 1-8 are in agreement with 0.09, 7.0, 15.0, 50.0, 100.0, 200.0, 300.0 and 400.0 μM of hydrazine. The inset shows the peak current plot as a concentration function of hydrazine within the range of 0.09-400.0 μM .

Analyzing Real Sample

The method illustrated above was used to evaluate DMOF-1/SPE usability for determining hydrazine in real samples in order to determine hydrazine in various water samples. Therefore, the standard addition technique was applied. Table 1 reports the results. Acceptable recoveries of hydrazine were observed, and reproducible results were shown with regard to the mean relative standard deviation (R.S.D.).

CONCLUSIONS

In this work, a method was suggested to create an

electrochemical sensor with a high-performance level used to determine hydrazine in aqueous solution in a sensitive manner. In aqueous solution of phosphate buffer, this modified electrode shows outstanding electrocatalytic behavior toward hydrazine oxidation. Moreover, a low detection limit (0.02 μM) and an excellent sensor performance with a wide linear range (0.09-400.0 μM) were reported as the features of the modified electrode under optimal conditions. In addition, the hydrazine was successfully determined by this modified electrode in different water samples, and proper recoveries were observed.

Table 1. The Application of DMOF-1/SPE for Determination of Hydrazine in Various Water Samples (n = 5). All Concentrations are in μM

Sample	Spiked	Found	Recovery (%)	R.S.D. (%)
River water	0	-	-	-
	5.0	4.9	98.0	3.3
	10.0	10.1	101.0	1.8
	15.0	15.4	102.7	2.3
	20.0	19.7	98.5	2.6
Tap water	0	-	-	-
	7.5	7.6	101.3	1.9
	12.5	12.2	97.6	3.1
	17.5	18.1	103.4	2.7
	22.5	22.1	98.2	2.4
Rain water	0	-	-	-
	7.0	6.9	98.6	2.5
	12.0	12.3	102.5	1.8
	17.0	16.8	98.8	3.2
	22.0	22.1	100.4	2.5

ACKNOWLEDGEMENTS

The authors acknowledge the financial support provided for this project (No. 98000010) by the Bam University of Medical Sciences, Bam, Iran and Kerman University of Medical Sciences, Kerman, Iran.

REFERENCES

- [1] T. Rebiś, M. Sobkowiak, G. Milczarek, J. Electroanal. Chem. 780 (2016) 257.
- [2] H. Hamidi, S. Bozorgzadeh, B. Haghghi, Microchim. Acta 184 (2017) 4537.
- [3] H. Mahmoudi-Moghaddam, H. Beitollahi, S. Tajik, I. Sheikhshoae, P. Biparva, Environ. Monit. Assess. 187 (2015) 407.
- [4] C. Saengsookwaow, R. Rangkupan, O. Chailapakul, N. Rodthongkum, Sens. Actuators B Chem. 227 (2016) 524.
- [5] M. Faisal, F.A. Harraz, A.E. Al-Salami, S.A. Al-Sayari, A. Al-Hajry, M.S. Al-Assiri, Mater. Chem. Phys. 214 (2018) 126.
- [6] A. Kalaivani, S.S. Narayanan, J. Mater. Sci.-Mater El. 29 (2018) 20146.
- [7] A.D. Smolenkov, O.A. Shpigun, Talanta 102 (2012) 93.
- [8] W. Siangproh, O. Chailapakul, R. Laocharoensuk, J. Wang. Talanta 67 (2005) 903.

- [9] A. Safavi, M.A. Karimi, *Talanta* 58 (2002) 785.
- [10] P. Ortega-Barrales, A. Molina-Díaz, M.I. Pascual-Reguera, L.F. Capitán-Vallvey, *Anal. Chim. Acta* 353 (1997) 115.
- [11] J.A. Oh, J.H. Park, H.S. Shin, *Anal. Chim. Acta* 769 (2013) 79.
- [12] K. Ghanbari, *Synth. Met.* 195 (2014) 234.
- [13] S. Esfandiari-Baghbamidi, H. Beitollahi, S. Tajik, *Anal. Bioanal. Electrochem.* 6 (2014) 634.
- [14] M. Afshari, M. Dinari, M.M. Momeni, *J. Electroanal. Chem.* 833 (2019) 9.
- [15] M. Hosseini-Ghalehno, M. Mirzaei, M. Torkzadeh-Mahani, *Microchim. Acta* 185 (2018) 165.
- [16] S.Z. Mohammadi, H. Beitollahi, S. Tajik, *Micro. Nano. Sys. Lett.* 6 (2018) 9.
- [17] D.W. Li, Y.T. Li, W. Song, Y.T. Long. *Anal. Methods* 2 (2010) 837.
- [18] J. Yang, J.H. Yu, J.R. Strickler, W.J. Chang, S. Gunasekaran, *Biosens. Bioelectron.* 47 (2013) 530.
- [19] H. Beitollahi, Z. Dourandish, S. Tajik, M.R. Ganjali, P. Norouzi, F. Faridbod, *J. Rare Earths.* 36 (2018) 750.
- [20] B. Rafiee, A.R. Fakhari, *Biosens. Bioelectron.* 46 (2013) 130.
- [21] S. Frutos-Puerto, C. Miró, E. Pinilla-Gil, *Sensors* 19 (2019) 279.
- [22] S. Esfandiari-Baghbamidi, H. Beitollahi, S. Tajik, R. Hosseinzadeh, *Int. J. Electrochem. Sci.* 11 (2016) 10874.
- [23] A. Özcan, D. Topçuoğulları, A.A. Özcan, *Sens. Actuators B Chem.* 284 (2019) 179.
- [24] M.M. Motaghi, H. Beitollahi, S. Tajik, R. Hosseinzadeh, *Int. J. Electrochem. Sci.* 11 (2016) 7849.
- [25] Y. Wei, A. Wang, Y. Liu, *Russ. J. Electrochem.* 54 (2018) 1141.
- [26] K.F. Chan, N.H. Lim, N. Shams, S. Jayabal, A. Pandikumar, N.H. Huang, *Mater. Sci. Eng. C* 58 (2016) 666.
- [27] B. Rafiee, A.R. Fakhari, M. Ghaffarzadeh, *Sens. Actuators B Chem.* 218 (2015) 271.
- [28] M.R. Ganjali, H. Beitollahi, R. Zaimbashi, S. Tajik, M. Rezapour, B. Larijani, *Int. J. Electrochem. Sci.* 13 (2018) 2519.
- [29] M.L. Yola, T. Eren, N. Atar, *Sens. Actuators B Chem.* 210 (2015) 149.
- [30] A.H. Touny, R.H. Tammam, M.M. Saleh, *Appl. Catal. B-Environ.* 224 (2018) 1017.
- [31] H. Soltani, H. Beitollahi, A.H. Hatefi-Mehrjardi, S. Tajik, M. Torkzadeh-Mahani, *Anal. Bioanal. Electrochem.* 6 (2014) 67.
- [32] T. Alizadeh, M.R. Ganjali, M. Akhoundian, P. Norouzi, *Microchim. Acta* 183 (2016) 1123.
- [33] A. Pahlavan, N. Rezaejad, H. Karimi-Maleh, M.R. Jamali, M. Abbasghorbani, H. Beitollahi, N. Atar, *Int. J. Electrochem. Sci.* 10 (2015) 3644.
- [34] L. Wang, R. Yang, J. Li, L. Qu, P.D.B. Harrington, *Sens. Actuators B Chem.* 215 (2015) 181.
- [35] M.R. Ganjali, Z. Dourandish, H. Beitollahi, S. Tajik, L. Hajiaghababaei, B. Larijani, *Int. J. Electrochem. Sci.* 13 (2018) 2448.
- [36] M.R. Akanda, M. Sohail, M.A. Aziz, A.N. Kawde, *Electroanalysis* 28 (2016) 408.
- [37] H. Mahmoudi-Moghaddam, S. Tajik, H. Beitollahi, *Food Chem.* 286 (2019) 191.
- [38] X. Hou, G. Shen, L. Meng, L. Zhu, M. Guo, *Russ. J. Electrochem.* 47 (2011) 1262.
- [39] M.R. Ganjali, H. Salimi, S. Tajik, H. Beitollahi, M. Rezapour, B. Larijani, *Int. J. Electrochem. Sci.* 12 (2017) 5243.
- [40] X.L. Jiang, R. Li, J. Li, X. He, *Russ. J. Electrochem.* 45 (2009) 772.
- [41] H. Beitollahi, S. Tajik, *Environ. Monit Assess.* 187 (2015) 257.
- [42] M. Xu, M. Ma, Y. Ma, *Russ. J. Electrochem.* 48 (2012) 489.
- [43] M. Peksa, J. Lang, F. Stallmach, *Microporous Mesoporous Mater.* 205 (2015) 11.
- [44] Y. Li, C. Huangfu, H. Du, W. Liu, Y. Li, J. Ye, *J. Electroanal. Chem.* 709 (2013) 65.
- [45] H. Hosseini, H. Ahmar, A. Dehghani, A. Bagheri, A. Tadjarodi, A.R. Fakhari, *Biosens. Bioelectron.* 42 (2013) 426.
- [46] L. Liu, Y. Zhou, S. Liu, M. Xu, *Chem. ElectroChem.* 5 (2018) 6.
- [47] A.J. Bard, L.R. Faulkner, *Electrochemical Methods, Fundamentals and Applications.* Wiley, New York, 2001.
- [48] N. Motakef-Kazemi, S.A. Shojaosadati, A. Morsali, J.

- Iran. Chem. Soc. 13 (2016) 1205.
- [49] O. Shekhah, Materials 3 (2010) 1302.
- [50] Q. Chen, X. Li, X. Min, D. Cheng, J. Zhou, Y. Li, Z. Xie, P. Liu, W. Cai, C. Zhang, J. Electroanal. Chem. 789 (2017) 114.